Structural Study of Methyl and *tert*-Butyl Phenylacetate Enolates in Solution: Spectroscopic Determination of Their *E* or *Z* Configuration

Jacques Corset,*,† Françoise Froment,† Marie-France Lautié,† Nicole Ratovelomanana,† Jacqueline Seyden-Penne,‡ Tekla Strzalko,‡ and Marie-Claude Roux-Schmitt‡

Contribution from the Laboratoire de Spectrochimie Infrarouge et Raman, CNRS, BP 28, 94320 Thiais, France, and Laboratoire des Carbocycles, associé au CNRS, ICMO, Université Paris-Sud, 91405 Orsay, France. *Received January 28, 1992. Revised Manuscript Received December 5, 1992*

Abstract: The structures of Li and K methyl and *tert*-butyl phenylacetate enolates **A,M** and **B,M** have been examined by IR and ^{13}C NMR spectroscopy in different solvents and solvent mixtures. In the IR, coupling of the 8a (or 8b) aromatic ring mode with the $\nu(C{=}O)$ stretching vibration allows assignment of the *E* (or *Z*) configuration to the corresponding enolate. The IR mode assignments are secured by specific deuteration of the phenyl or methyl moieties in methyl phenylacetate. Free anions **1A** and **1B** and solvent- and cryptand-separated pairs **1A,[M]** and **1B,[M]** exhibit the *Z* geometry. In THF, when M = Li, two species **2A,Li** and **3A,Li** or **2B,Li** and **3B,Li** in slow equilibrium on the NMR time scale are observed, both having the *E* configuration. Monomeric ion pairs **2A,Li** or **2B,Li**, which are primarily generated, are slowly associated into dimeric, tight ion pairs **3A,Li** or **3B,Li**, the position of the equilibrium depending upon the nature of the enolate (Me or *t*-Bu) and its concentration. The addition of HMPA to **2A,Li** and **2B,Li** or **3A,Li** and **3B,Li** THF solutions induces an $E \rightarrow Z$ isomerization, leading to Li-HMPA solvates **2'A,Li** and **2'B,Li** which have been characterized by low-temperature ^{31}P NMR. In this system, lithium enolate trapping in THF by Me_3SiCl is unreliable as a method for assigning their *E* geometry.

Ester enolate chemistry has recently been the subject of intense investigation, namely, aldol-type reactions,[1,2] substituted amino acid[3] or β-lactam[4] synthesis, or Michael additions.[3c,5] Such is also the case for their related silyl ketene acetals, as the Ireland–Claisen rearrangement of these species has become popular in organic synthesis.[6] Determination of the *Z* or *E*[7] configuration of enolates and ketene acetals has proven to be of prime importance in diastereoselection.[1-6,8]

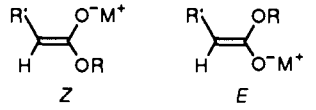

The X-ray crystallographic determination of Li *tert*-butyl propionate enolate dimer[9] has shown its geometry to be *E* (R' = Me, R = *t*-Bu) in the solid state; this geometry is maintained in THF solution as deduced from the results of enolate trapping by *t*-BuPh$_2$SiCl and X-ray analysis of the corresponding ketene acetal.[10] However, in THF/HMPA solution, the *Z* isomer is predominantly generated, most likely under kinetic control.[8a,b]

The geometry of lithium methyl phenylacetate enolates **A,Li** has been examined in solution:[2,8a] as inferred from trapping experiments by trialkylsilyl chlorides, it appears that, depending on the base, solvent, and temperature, different *Z*/*E* mixtures or only the *Z* isomer is formed. However, the reliability of assigning enolate geometry by such a method has been questioned in several instances.[8b,11-14] Our group has recently examined the reactivity of these ester enolates **A,M** and **B,M** toward alkyl 4-bromo-4-methylpent-2-enolates.[15]

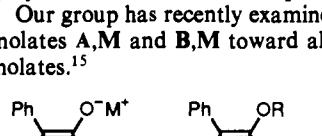

A, M: R = Me
$M^+ = Li^+$ or K^+

B, M: R = *t*-Bu
$M^+ = Li^+$ or K^+

In order to interpret further the regio- and stereoselectivities observed and examine the relevance of trapping experiments by trialkylsilyl chlorides, we investigated by IR and NMR spectroscopy the structures of these enolate species **A,M** and **B,M** in the conditions under which the chemical study and some trapping experiments were performed.

Enolates may exist in solution as aggregates, tight ion pairs, solvent- or cryptand-separated ion pairs, and free ions which are in equilibrium.[16-20] Different solvent and concentration conditions

† Laboratoire de Spectrochimie Infrarouge et Raman.
‡ Laboratoire des Carbocycles.

(1) Evans, D. A.; Nelson, J. O.; Taber, T. R. *Top. Stereochem.* **1983**, *13*, 1. Heathcock, C. H. *Asymmetric Synth.* (Morrison, J. D., Ed.) **1984**, *3*, 111.
(2) Kiyooka, S. I.; Kandori, K.; Fujiyama, R.; Suzuki, K. *Kochi Daigaku Rigakubu Kiyo, Kagaku Ser. C* **1985**, *6*, 1 and references cited therein; *Chem. Abstr.* **1985**, *103*, 141111u.
(3) (a) O'Donnell, M. J.; Bennett, W. D.; Wu, S. *J. Am. Chem. Soc.* **1989**, *111*, 2353 and references cited therein. (b) El Achqar, A.; Roumestant, M. L.; Viallefont, P. *Tetrahedron Lett.* **1988**, *29*, 2441 and references cited therein. (c) Yamaguchi, M.; Torisu, K.; Minami, T. *Chem. Lett.* **1990**, 377 and references cited therein.
(4) (a) Van der Steen, F. H.; Kleijn, H.; Jastrzebski, J. T. B. H.; Van Koten, G. *Tetrahedron Lett.* **1989**, *30*, 765 and references cited therein. (b) Jastrzebski, J. T. B. H.; Van Koten, G. *Inorg. Chim. Acta* **1988**, *142*, 169. (c) Van der Steen, F. H.; Boersma, J.; Spek, A. L.; Van Koten, G. *Organometallics* **1991**, *10*, 2467. (d) Van der Steen, F. H.; Kleijn, H.; Jastrzebski, J. T. B. H.; Van Koten, G. *J. Org. Chem.* **1991**, *56*, 5147.
(5) (a) Oare, D. A.; Heathcock, C. H. *Top. Stereochem.* (Eliel, E. L., Wilen, S., Eds.) **1989**, *19*, 227. (b) Oare, D. A.; Heathcock, C. H. *J. Org. Chem.* **1990**, *55*, 157 and references cited therein. (c) Viteva, L.; Stefanovsky, Y. *J. Chem. Res., Synop.* **1990**, 232. (d) Viteva, L.; Stefanovsky, Y. *Tetrahedron Lett.* **1990**, *31*, 5649.
(6) (a) Blechert, S. *Synthesis* **1989**, 71. (b) Ziegler, F. E. *Chem. Rev.* **1988**, *88*, 1423.
(7) In this article, for the sake of simplicity, we shall adopt a single *Z* or *E* notation for enolates and ketene acetals[5a,b] so that OLi will have, as OK and $OSiR_3$, a higher priority over OR; thus, to any *Z* enolate will correspond a *Z* ketene acetal and vice versa.
(8) (a) Ireland, R. E.; Mueller, R. M.; Willard, A. K. *J. Am. Chem. Soc.* **1976**, *98*, 2868. (b) Ireland, R. E.; Wipf, P.; Armstrong, J. D. *J. Org. Chem.* **1991**, *56*, 650.
(9) Seebach, D.; Amstutz, R.; Laube, T.; Schweizer, W. B.; Dunitz, J. D. *J. Am. Chem. Soc.* **1985**, *107*, 5403.
(10) Babston, R. E.; Lynch, V.; Wilcox, C. S. *Tetrahedron Lett.* **1989**, *30*, 447.
(11) Corey, E. J.; Gross, A. W. *Tetrahedron Lett.* **1984**, *25*, 495.
(12) Spears, G. W.; Caufield, C. E.; Still, W. C. *J. Org. Chem.* **1987**, *52*, 1226.
(13) (a) Krause, V.; Lauer, W.; Meier, H. *Chem. Ber.* **1989**, *122*, 1719. (b) Meier, H.; Lauer, W.; Krause, V. *Chem. Ber.* **1988**, *121*, 1109.
(14) Beutelman, H. P.; Xie, L.; Saunders, W. H. *J. Org. Chem.* **1989**, *54*, 1703.
(15) (a) Roux-Schmitt, M. C.; Petit, A.; Sevin, A.; Seyden-Penne, J.; Anh, N. T. *Tetrahedron* **1990**, *46*, 1263. (b) Roux-Schmitt, M. C.; Sevin, A.; Seyden-Penne, J. *Bull. Soc. Chim. Fr.* **1990**, 857. (c) Sevin, A.; Seyden-Penne, J.; Boubeker, K. *Tetrahedron Asymmetry* **1991**, *2*, 1107.

0002-7863/93/1515-1684$04.00/0

will be selected in order to shift these equilibria toward one predominating species, characterized by its IR and NMR (^{13}C, occasionally ^{31}P and ^{7}Li) spectra. The structural information will be deduced both from the normal IR mode frequency displacements and large intensity variations as well as from NMR chemical shifts when going from the neutral precursors $C_6H_5CH_2COOCH_3$ (**A**) or $C_6H_5CH_2COOC(CH_3)_3$ (**B**) to the corresponding enolates **A**,**M** or **B**,**M**. In order to secure the IR vibrational assignments, the spectra of partially deuterated methyl phenylacetates $C_6D_5CH_2COOCH_3$ (**A**-d_5) and $C_6H_5CH_2COOCD_3$ (**A**-d_3) as well as those of the corresponding enolates **A**,**M**-d_5 and **A**,**M**-d_3 will be analyzed.

At low concentration, in highly polar solvents or in low-polarity solvents when using cation complexing agents such as cryptands, free anions **1A** or **1B** or solvent- and cryptand-separated ion pairs **1A**,[M] or **1B**,[M] should be the predominant species.

In pure THF tight ion pairs are expected, which can be either monomeric[21] or in various aggregation states:[20] indeed, two kinds of species **2A**,Li and **3A**,Li or **2B**,Li and **3B**,Li could be characterized, their relative amounts being dependent upon their concentration and generation conditions (vide infra). In THF/toluene mixtures (40:60, v:v), more aggregated species **4A**,**M** or **4B**,**M** might be expected. Finally, the addition of potent cation-solvating agents such as HMPA to **A**,Li or **B**,Li solutions might lead to the formation of externally solvated ion pairs **2'A**,Li or **2'B**,Li at low HMPA concentration[19,20] and to solvent-separated ion pairs **1A**,[M] and **1B**,[M] or free ions **1A** and **1B** at higher HMPA concentrations.

In connection with this spectroscopic study, the generation and the structure of the corresponding trimethylsilyl ketene acetals will be reexamined, including NOE experiments,[22] and the results will be compared to previous literature data.[2,8a,23]

Results and Discussion

Enolate Generation. The different bases (1 M LHMDS in THF, 1.6 M *n*-BuLi in hexane, 0.5 M KHMDS in toluene, and freshly sublimated *t*-BuOK) were used in slight excess (1.2–1.5 equiv).[24] Therefore, the resulting anionic species were present in the following solvents or solvent mixtures: pure THF, pure DMSO, THF/hexane, THF/toluene, THF/HMPA, THF/DMSO, DMSO/toluene. The final solutions were usually 0.2–0.25 M unless indicated otherwise, and the disappearance of the ν(C=O) IR absorption of the neutral esters **A** and **B** in these solutions proved that the enolates were totally generated (Figure 1c,d). Due to the low pK_a of phenylacetic acid esters (pK_a = 22.6)[26] and electronic delocalization into the aromatic ring which stabilizes the anionic species as will be shown below, deprotonation could be performed by LHMDS at room temperature as all of these enolates were stable in such conditions for several hours.[27] It has indeed been checked by an acidic quench (10% HCl) of all of the enolates that the starting phenylacetates **A** or **B** were totally recovered after reprotonation; this proves that no enolate self-condensation took place under our experimental conditions.[8b,28]

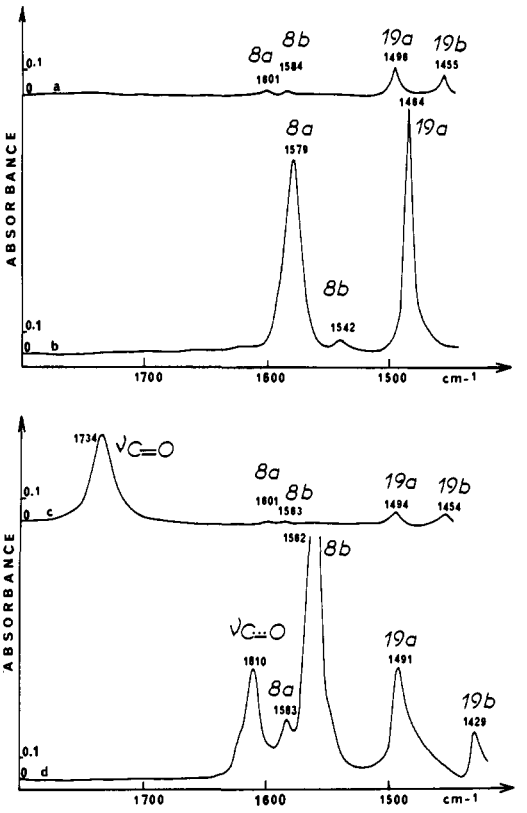

Figure 1. Intensity enhancements of the skeleton benzenic ring modes 8a, 8b, 19a, and 19b in the infrared absorption spectra of the carbanionic species of phenylacetonitrile (b) and methyl phenylacetate (d) generated with *t*-BuOK in DMSO. The starting compound spectra are reported for $C_6H_5CH_2CN$ (a) and $C_6H_5CH_2COOCH_3$ (c) in DMSO solution. The concentrations of the compounds are 0.43 (a), 0.21 (c), and 0.25 M (b and d). The cell thickness is 0.003 cm. The spectra are obtained at 26 °C.

The use of *t*-**BuOK** raised two problems: (a) In pure THF, the formation of **A**,**K** and **B**,**K** required the addition of [2.2.2] cryptand to prevent precipitation. (b) In DMSO, when using not freshly sublimated *t*-**BuOK**, methyl phenylacetate was transformed into potassium phenylacetate through hydrolysis of the ester by KOH. The reactivity of $C_6H_5CH_2COOK$ toward methyl 4-bromo-4-methylpent-2-enoate was totally different from that of **A**,**K**.[29]

Infrared and Raman Spectra of Alkyl Phenylacetates A or B in Solution. The IR spectra of the neutral precursors **A**, **A**-d_3, and **A**-d_5 have been recorded as pure liquids (Table I, entries 1, 4, and 7) and in THF and DMSO solutions (Table II, entries 10 and 11), as have those of **B** (Table III, entries 1 and 2), at 0.25 M concentration. The Raman spectrum of **A**-d_5 is also reported (Table I, entry 8). The assignments of the bands are given in terms of group frequencies. The observed vibrations of the benzenic ring are mainly those of the five stretching carbons of the skeleton: 8a, 8b, 19a, 19b, and 14 according to the Wilson notation.[31a] They show a small shift to lower frequencies in the d_5 compound due to a slight contribution of the δCH/CD coordinates to these modes

(16) Jackman, L. M.; Scarmoutzos, L. M. *J. Am. Chem. Soc.* **1987**, *109*, 5348.
(17) Jackman, L. M.; Smith, B. D. *J. Am. Chem. Soc.* **1988**, *110*, 3829.
(18) Jackman, L. M.; Szeverenyi, N. M. *J. Am. Chem. Soc.* **1977**, *99*, 4954.
(19) Jackman, L. M.; Lange, B. C. *J. Am. Chem. Soc.* **1981**, *103*, 4494.
(20) Seebach, D. *Angew. Chem., Int. Ed. Engl.* **1988**, *27*, 1624.
(21) Kaufman, M. J.; Gronert, S.; Bors, D. A.; Streitwieser, A. *J. Am. Chem. Soc.* **1987**, *109*, 602.
(22) (a) Guanti, G.; Banfi, L.; Narisano, E.; Scolastico, C. *Tetrahedron* **1988**, *44*, 3671. (b) Van der Steen, F. H.; Boersma, J.; Spek, A. L.; Van Koten, G. *J. Organomet. Chem.* **1990**, *390*, C21.
(23) Burlachenko, G. S.; Baukov, Y. I.; Dzherayan, T. G.; Lutsenko, I. F. *Zh. Obshch. Khim.* **1975**, *45*, 81; *J. Gen. Chem. USSR (Engl. Transl.)* **1975**, *45*, 73.
(24) The amount of base used to generate enolates differs from case to case in the literature. Saunders[14] recommends a 3-fold amount of base to avoid $E \rightleftarrows Z$ equilibrations; nevertheless, in such a situation, mixed aggregates may be formed.[25] On the other hand, Ireland[8b] observes a different stereoselectivity in LDA deprotonation of methyl propionate according to the base:ester ratio, although no similar effect is reported when using LHMDS or KHMDS. That is one of the reasons why LDA was not used here.
(25) Williard, P. G.; Hintze, M. S. *J. Am. Chem. Soc.* **1990**, *112*, 8602.
(26) Bordwell, F. G. *Acc. Chem. Res.* **1988**, *21*, 456.
(27) In aliphatic series, only *t*-Bu ester enolates are stable at room temperature: Dieter, R. K.; Fishpaugh, J. R. *J. Org. Chem.* **1988**, *53*, 2031.
(28) Turner, J. A.; Jacks, W. S. *J. Org. Chem.* **1989**, *54*, 4229.
(29) The reaction of $PhCH_2COOMe$ + old *t*-BuOK in DMSO with $BrMe_2CCH{=}CHCO_2Me$ leads to, instead of $Me_2C{=}CHCH(CO_2Me)CH(CO_2Me)Ph$, the β-elimination product $H_2C{=}C(Me)CH{=}CHCO_2Me$ identified by comparison with an authentic sample.[30] It has been checked that preformed $PhCH_2COOK$ in DMSO gives the same product (see Experimental Section).
(30) Etemad-Moghadam, G.; Seyden-Penne, J. *Tetrahedron* **1984**, *40*, 5153.
(31) (a) Wilson, E. B.; Decius, J. C.; Cross, P. C. *Molecular Vibrations*; McGraw-Hill: New York, 1955. (b) Scherer, J. A. *Planar Vibrations of Benzenes*; The Dow Chemical Company: Midland, MI, 1963.

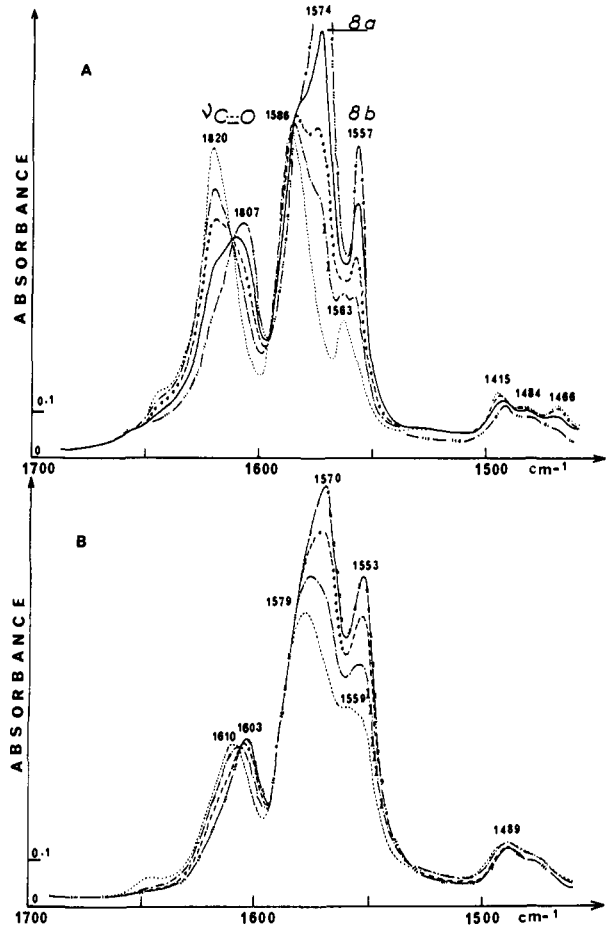

Figure 2. Evolution with time of the infrared absorption spectra of carbanionic species **2A,Li** (A) or **2B,Li** (B) generated with LHMDS in THF solutions toward **3A,Li** or **3B,Li**. (A) —·—, t_0 = 5 min at room temperature; —, t_1 = 2 h; - - -, t_2 = 3 h; —, t_3 = 4 h; ···, t_4 = 7 h. (B) —·—, t_0 = 5 min; - - -, t_1 = 30 min; —, t_2 = 1 h; ···, t_3 = 1 h 45 min. The spectrometer temperature varies from 26 to 32 °C.

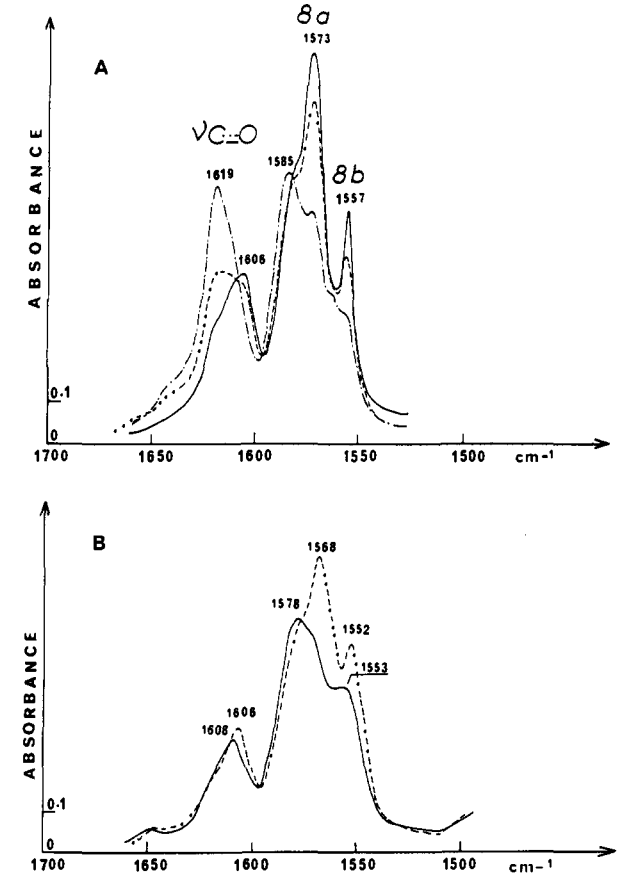

Figure 3. Influence of dilution on the infrared absorption spectra of carbanionic species **2A,Li** (A) or **2B,Li** (B) and **3A,Li** or **3B,Li** generated with LHMDS (A, B) in THF solutions. The concentrations are as follows: —, 0.25 (A, B); - - -, 0.05 (A, B); -·-, 0.025 M (A). The cell thickness is 0.003 cm or 0.020 cm for dilute solution. The ordinate scale is enhanced by a 2.5 factor for —·—. The time variation between the spectra scanning of the concentrated and the more dilute solution is less than 2 h. The spectra are obtained at 26 °C.

as expected. In this region is also expected at least one of the ν(C–C–C) modes of the bridge between the phenyl and the C(O)OR ester group. One of them, as is usually found in monosubstituted benzenic compounds, couples with an in-plane ring deformation vibration 1 or 12 and will be called "e". The other ν(C–C–C) mode is probably located under 1000 cm^{-1}. Their frequencies are only slightly lowered in **A**-d_5 relative to **A**. The other modes observed for the phenyl ring are mainly δ(CH) in-plane bending vibrations, 3, 9a, 9b, 18a, 18b,[31a] which shift to lower frequencies in **A**-d_5. All of these band frequencies are very close to those of toluene, for which a normal mode calculation has been performed.[32]

The assignments of the ester group vibrations are given by comparison with those of methyl acetate[33,34a] for **A** and *tert*-butyl formate[35] for **B**. The backbone of the ester group is generally considered to be planar due to the partial double-bond character of the C—O bond adjacent to the C=O group: the stretching frequency of this bond is indeed observed at 1255 cm^{-1} in **A** and at 1274 cm^{-1} in **A**-d_3 (Table I, entries 1 and 4). Methyl esters usually exhibit an s-cis conformation relative to the O—CH_3 bond, while for *tert*-butyl formate s-cis and s-trans conformations in equilibrium are observed.[35] Such conformations might also exist in the present case. They have not been examined as most of their characteristic vibrational modes appear at frequencies lower than the transparency limit of the CaF_2 cells. The OCH_3 and OCD_3 bending and rocking modes are easily assigned through comparison of the spectra of **A** and **A**-d_3 (Table I, entries 1 and 4). The $\delta(CH_2)$ and $\omega(CH_2)$ deformation vibrations show a main band with a shoulder or a doublet. Although the $\delta(CH_2)$ mode can be partly overlapped by a $\delta_a(OCH_3)$ mode expected around 1439 cm^{-1},[33] it appears as a doublet for **A**-d_3 (Table I, entry 4). The fact that the $\delta(CH_2)$ mode is a doublet for **A**-d_3 is related to the existence of two conformers around the C–C single bond α to the C=O group, as already observed.[34b]

Infrared and NMR Spectra of Enolate Species: Ionic Association. The assignments of all of the absorptions observed above 1000 cm^{-1} for lithium phenylacetate enolates in THF and of the main IR vibrational modes of the other species are given in Tables I–III and some of their spectra in Figures 1–6. The main ^{13}C NMR parameters of some of them are in Table IV next to those of neutral precursors **A** and **B**, as well as a few results from the literature[36] for comparison. The ^{31}P and ^{7}Li NMR parameters of **2′A,Li** and **2′B,Li** solutions in THF/HMPA are given in the text.

Before the peculiar features of each species are described, the main meaningful modifications of the spectra related to those of the neutral precursors will be summarized. The IR spectra show the following: (1) a low-frequency shift of the ν(C···O) vibrations which appear around 1600–1620 cm^{-1} in **A,M** and **B,M** characteristic of partial double-bond character as in other ester

(32) Lalau, G.; Snyder, R. G. *Spectrochim. Acta* **1971**, *27A*, 2073.
(33) George, W. O.; Houston, T. E.; Harris, W. C. *Spectrochim. Acta* **1974**, *30*, 1035.
(34) (a) Moravie, R. M.; Corset, J. *J. Mol. Struct.* **1976**, *30*, 113. (b) Moravie, R. M.; Corset, J. *J. Mol. Struct.* **1975**, *24*, 91.
(35) Omura, Y.; Corset, J.; Moravie, R. M. *J. Mol. Struct.* **1979**, *52*, 175 and references cited therein.
(36) (a) Bradamante, S.; Pagani, G. *J. Chem. Soc., Perkin Trans. 2* **1986**, 1035. (b) Vogt, H. H.; Gompper, R. *Chem. Ber.* **1981**, *114*, 2884.

Table I. IR and Raman[a] Frequencies (cm^{-1}) and Assignments of Methyl Phenylacetates **A**, **A**-d_3, and **A**-d_5 (Pure Liquid) and Lithiated Anionic Species in THF Solution **2A** or **3A**,Li and **2A** or **3A**,Li-d_3, -d_5 Generated with LHMDS[b]

	$C_6H_5CH_2COOCH_3$			$C_6H_5CH_2COOCD_3$			$C_6D_5CH_2COOCH_3$			
	1[c] **A**	2 **2A**,Li	3 **3A**,Li	4 **A**-d_3	5 **2A**.Li-d_3	6 **3A**,Li-d_3	7 **A**-d_5	8 **A**-d_5[a]	9 **2A**,Li-d_5	10 **3A**,Li-d_5
ν(C=O)	1736s			1734s			1737s	1737m		
ν(C···O)		1607m	1620s		1605m	1617m			1594s	1615s
							1580w			
8a	1601m	1574s	1586s	1601w	1575s	1584s	1568w	1570s	1551s	1556m
8b	1583w	1557m	1563m	1583w	1556m	1561m		(1559)	1523w	1527w
								(1551)		
19a	1494m	1492w 1481w	1495w 1484w	1494m	1493m 1481m	1493m 1481m	1383m	1388w	1387w	1387w
19b	1453m	1444m (1437)	(1450) 1438m	1453m	(1448) 1442m	1448m			1370w	1370w
$\delta(CH_2)$	1433m (1415)			1429w 1414w			1434m 1416w	1434m (1418)		
$\delta_a(OCX_3)$		1469w	1469m	1086s	1105m	1105m	1452w	1457w	1488w (1450)	1488w 1470w (1450)
$\delta_s(OCX_3)$									1439m	1439m
ν_a(C-C-C)		1413w 1343m	1411m 1343w		1413w 1344m	1413m 1344w			1425w 1345m	1425m 1345w
$w(CH_2)$	1341m (1327)			1347m 1327w			1349m 1320m			
14	1300m	1322m	1324w	1303m	1323w	1323w	1302m	1296m	(1323)	1323w
ν_s(C-C-C)		1300m	1300w		1309m	1300w			1311m	
ν(C-OCX_3)	1255s	(1294) 1281w	(1292)	1274m	(1294)	(1294)	1256m	1251w	1291m (1279)	1294w 1279w
"e"	1220m	1228w	1228w	1226m	1228m	1228w	1196m	1208w	1228m	1228w
$\rho_{\parallel}(OCX_3)$		1214w	1212w		1046m	1046m	1162m	1187w	1210w 1181m	1200m 1181m
9a	1190m	1189m	1190m	1178m	1189m	1162m				
9b	1159s	1176m	1176w	(1162) 1146w	1176m	1176m				
$\rho_{\perp}(OCX_3)$	(1138)	(1144)w 1138m	1144m (1137)m		992w 978w	992w 978m	1146m	1146s 1136s	1157w (1125)	1128m
							(1115)	(1114)		
18b	1074m			1053w				1074w		
3							1046m	1046m		
18a	(1029)			1030w			1013m			
12	1012m			1018w			1004m	1005m		
	(999)			1003w						

[a] Raman frequencies (cm^{-1}). C = 0.25 M. [b] The intensities of the bands are given as follows: strong, s; mean, m; weak, w. The frequencies given between brackets correspond to shoulders. [c] Entry numbers.

enolates[37] and (2) a low-frequency shift as well as an intensity increase of the 8a, 8b, 19a, and 19b phenyl ring vibrations similar for the h_5 and d_5 species, as already observed in phenylacetonitrile carbanionic species[38] (Figure 1a,b). When generating enolates **A**,**M**, either 8a or 8b mode intensity is more greatly increased than that of the 19a mode (Figures 1c,d and 4a,b); this is interpreted as a mixing of either the 8a or 8b mode with the ν(C···O) stretching one, depending on whether the geometry of the enolate is *E* or *Z*.

Indeed, in the IR spectrum of phenylacetonitrile,[38] the skeleton benzenic ring modes 8a, 8b, 19a, and 19b, involving mainly the displacement of the carbon atoms as shown in Scheme I, have low IR intensity relative to the low polarity of the benzene ring according to calculations by Scherer[31b] (Figure 1a). In the corresponding anion (Figure 1b), the charge delocalization into the aromatic ring leads to a polarization of its C···C bonds, thus inducing a large intensity increase in the corresponding IR modes as previously noted.

Taking into account electronic charge delocalization when going from neutral phenylacetates to anionic species leading to the phenyl ring polarization and normal mode change, we observe the coupling of the 8a and 8b phenyl ring modes with the C···O stretching coordinate, the expected isolated frequencies of which being very close. If the enolate exhibits the *Z* configuration (Scheme I), the C···O stretching coordinate will not be far from orthogonal to the C_2 phenyl ring axis along which the variation of the μ_a dipole is oriented during the 8a or 19a vibration mode. Therefore, the

Scheme I

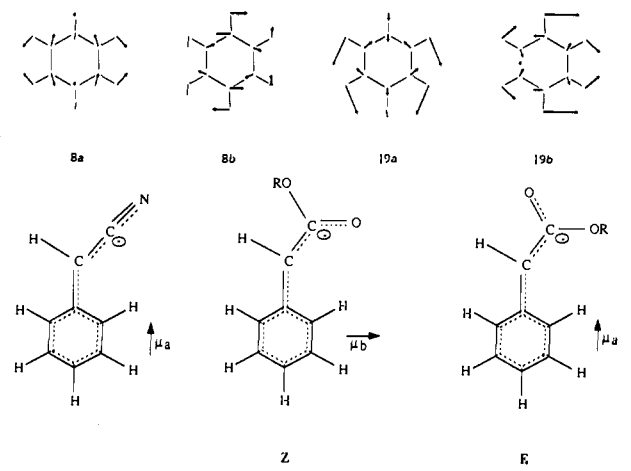

C···O stretching coordinate, being nearly parallel to μ_b, will mainly couple to the 8b mode, greatly increasing its intensity. This mixing leads to two new modes that, for the sake of clarity, will still be called ν(C···O) and 8b. Conversely, if the enolate is in the *E* configuration, for similar reasons a mixing of the ν(C···O) with 8a, thus inducing a large intensity increase of this absorption, will occur.

A strong increase in the C–C–C bridge stretching frequencies, which appear between 1410 and 1340 cm^{-1} for ν_a(C–C–C) and at 1300 cm^{-1} for ν_s(C–C–C) as quoted in the previous related study[38] (one of these modes is coupled with the 1 or 12 benzenic

(37) Corset, J. *Pure Appl. Chem.* **1986**, *58*, 1133.
(38) Croisat, D.; Seyden-Penne, J.; Strzalko, T.; Wartski, L.; Corset, J.; Froment, F. *J. Org. Chem.* **1992**, *57*, 6435.

Table II. Main IR Frequencies (cm^{-1}) and Assignments of $C_6H_5CH_2COOCH_3$ A and $C_6D_5CH_2COOCH_3$ A-d_5 and Anionic Species A,M and A,K-d_5 in Solution[a]

	1[g] A THF	2 A DMSO	3 1A,K[b] [2.2.2] THF	4 1A,K[b] DMSO	5 1A,Li[c] THF/HMPA (32:68, v:v)	6 1A,Li[c,e] THF/DMSO (27:73, v:v)	7 1A,K[d,f] DMSO/tol (40:60, v:v)	8 2'A,Li[c] THF/HMPA (80:20, v:v)	9 4A,K[d] THF/tol (40:60, v:v)	10 A-d_5 THF	11 A-d_5 DMSO	12 1A,K-d_5[b] [2.2.2] THF	13 1A,K-d_5[b] DMSO	14 1A,K-d_5[d,f] DMSO/tol (40:60, v:v)	15 4A,K-d_5[d] THF/tol (40:60, v:v)
ν(C=O)	1742s	1734s								1741s	1733s				
ν(C=O)			(1623)m	(1623)	1622m	(1622)	(1624)	(1622)							
			1610m	1610m	1615m	1612m	1610m	1613m	1604m			1610s	1603s	1604s	1592s
						(1590)		(1590)		1580w	1578w				
8a	1603w	1601w	1581w	1583w	(1579)	(1584)	1586w		1567s	1567w	1567w	(1544)	(1545)	(1545)	
8b	1585w	1583w	1562s	1562s	1563s	1565s	1562s	1567s	1551s			1535s	1537s	1537s	1545s
						(1552)	(1549)	(1551)				(1527)	(1527)	(1528)	1519s
19a	1496m	1494m	1490m	1491m	1491m	1493m	1491m	1493m	1485m	1383w	1384w	1376w*	1376w*	1367w	1366m
									1467w				1356m*	1353m	1347w
19b	1455m	1454m	1443w			(1432)	1457w		1449m					1329w	
			1425m	1429w		1425m	1429m	1434w	(1439)					1312w	

[a] The intensities of the bands are given as follows: strong, s; mean, m; weak, w. The frequencies given between brackets correspond to shoulders. * Bands possible overlapped by a band of t-BuOH. The bases used are: [b] t-BuOK. [c] LHMDS. [d] KHMDS. [e] 2'A,Li is also present. [f] 2'A,K or 2'A,K-d_5 is also present. C = 0.25 M. [g] Entry numbers.

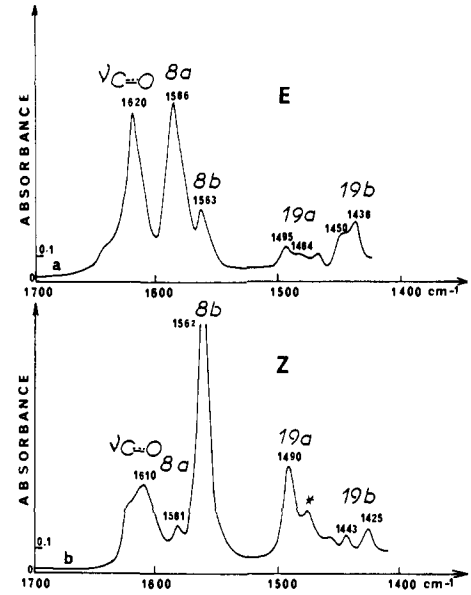

Figure 4. *E* and *Z* configurations of the enolates. Infrared absorption spectra of carbanionic species **3A,Li** (a) generated with LHMDS in THF solution and **1A,K** (b) generated with *t*-BuOK in THF solution in the presence of 1.2 equiv of [2.2.2] cryptand. The concentrations are 0.25 M. The cell thickness is 0.003 cm. * indicates the absorption band partially due to the vibration frequency of [2.2.2] cryptand (b) unsubtracted from solution spectra. The spectra are obtained at 26 °C.

in-plane mode, resulting in a mode designated "e"), is characteristic of charge delocalization into the phenyl ring. Some absorptions of the OCH_3 and OCD_3 groups, as well as some of the phenyl ring or C–C–C vibrations, appear as doublets in a few cases; they are probably due to the existence of conformers around the C–O alkyl bonds (vide infra).

The main ^{13}C NMR parameter variations are as follows: (1) positive C_α shifts whose values vary according to anion–cation interactions[39-41] and (2) negative C_4 shifts indicative of charge delocalization into the phenyl ring (they also depend upon anion–cation interactions, and their magnitudes are similar to those of phenylacetone enolates, depending on the cation and the solvent).[39,40]

Free Ions and Solvent- or Cryptand-Separated Ion Pairs: 1A or 1B and 1A,[M] or 1B,[M]. The IR spectra of **A,M** or **B,M** species were obtained under the following conditions: M = K [2.2.2] in THF (Table II, entry 3, and Table III, entry 5, Figure 4b); M = K in DMSO (Table II, entry 4, and Table III, entry 6); M = Li in DMSO or in THF/HMPA (32:68, v:v) (Table II entries 5 and 6, and Table III, entries 7 and 8, Figure 6d). These spectra are very similar. They are assigned to free ions **1A** or **1B** and solvent- or cryptand-separated ion pairs **1A**,[M] or **1B**,[M].

These IR spectra exhibit the following features. A strong ν(C⋯⋯O) absorption is observed around 1610 cm^{-1} which is slightly shifted when going from **1A** to **1A**-d_5 (Table II, entries 4 and 13). This band appears as a doublet or with a shoulder around 1623 cm^{-1} for **1A**,[M]. A weak absorption around 1583 cm^{-1}, shifted to around 1545 cm^{-1} for **1A**,[M]-d_5, is assigned to the 8a phenyl ring mode. A strong absorption around 1562 cm^{-1} for **1A**,[M] and 1559 cm^{-1} for **1B**,[M] (shifted to 1535 cm^{-1} for **1A**,[M]-d_5) is assigned to the 8b phenyl ring mode. The 19a mode has its frequency less shifted than the 8a one; it appears as a mean intensity band around 1490 cm^{-1}, while the 19b one is more frequency shifted, similar to 8a and 8b, and gives rise to a mean or weak band in the 1420–1443 cm^{-1} region, sometimes showing a doublet or a shoulder in **1A**,[M]. These data lead us to assign

(39) House, H. O.; Prabhu, A. V.; Philips, W. V. *J. Org. Chem.* **1976**, *41*, 1209.
(40) Noyori, R.; Nishida, I.; Sakata, J. *J. Am. Chem. Soc.* **1983**, *105*, 1598.
(41) O'Brien, D. H. In *Comprehensive Carbanion Chemistry*; Buncel, E., Durst, T., Eds.; Elsevier: Amsterdam, 1980; Part A, Chapter 6.

Table III. Main IR Frequencies (cm^{-1}) and Assignments of *tert*-Butyl Phenylacetate **B** and Anionic Species **B,M** in Solution[a]

	1[h] **B** THF	2 **B** DMSO	3 **2B,Li**[b] THF	4 **3B,Li**[b] THF	5 **1B,K**[c] [2.2.2] THF	6 **1B,K**[c] DMSO	7 **1B,Li**[b] THF/HMPA (32:68, v:v)	8 **1B,Li**[b,f] THF/DMSO (27:73, v:v)	9 **2'B,Li**[b,g] THF/HMPA (80:20, v:v)	10 **3B,Li**[d] THF/hex (80:20, v:v)	11 **4B,K**[e] THF/tol (45:55, v:v)
ν(C=O)	1733s	1725s									
ν(C···O)			1603m	1610m	1610m	1605m	1612m	1606m	1605m	1610m	1601m
8a	1602w	1601w	1570s	1579s		1586w				1583s	1567s
8b	1584w	1583w	1553m	1559m	1559s	1556s	1560s	1560s	1563s	1562m	1549s
									1549w	(1552)	
19a	1495m	1496m	1489w	1489w	1491m	1491m	1491m	1492m	1491m	1491w	1485w
19b	1454m	1454m	1440m	1442m	1443m		1439w		1439m	1441m	1443m

[a] The intensities of the bands are given as follows: strong, s; mean, m; weak, w. The frequencies given between brackets correspond to shoulders. The bases used are. [b] LHMDS. [c] *t*-BuOK. [d] *n*-BuLi. [e] KHMDS. [f] **2'B,Li** is also present. [g] **1B,Li** is also present. [h] Entry numbers.

Table IV. Main ^{13}C NMR Parameters of Ester Enolates **A,M** and **B,M** in 0.25 M Solution ($\Delta\delta$ in parentheses)[a]

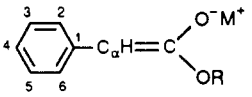

compd or species	M	solvent	C_α	CO	C_4	R
$PhCH_2COOMe$ **A**		THF	41.0	171.4	127.1	51.4
		DMSO	40.7	172.0	127.2	51.9
1A	Na[29b]	HMPA[b]	67.7	166	111.7	47.8
1A	Na[29a]	DMSO[c]	67.1		113.3	
			(+26.4)		(−13.9)	
1A	Li	DMSO/THF (70:30)	66.9	164.4	112.8	47.3
			(+26.2)	(−7.6)	(−14.4)	(−4.6)
1A	K	DMSO[c]	66.3	164.6	112.2	47.1
			(+25.6)	(−7.4)	(−15.0)	(−4.8)
2'A	Li	THF/HMPA (80:20)		166.7	114.1	49.4
				(−4.7)	(−13.0)	(−2.0)
4A	K	THF/toluene (50:50)	66.5	166.0	118.4	53.5
			(+25.5)	(−5.4)	(−8.7)	(+2.1)
2A	Li	THF	74.7	166.0	117.7	49.8
			(+33.7)	(−5.4)	(−9.4)	(−1.6)
3A	Li	THF	70.3	166.1	120.1	53.7
			(+29.3)	(−5.3)	(−7.0)	(+2.3)
$PhCH_2COOtBu$ **B**		THF	42.7	170.5	127.1	80.2; 27.9
		DMSO	40.7	169.5	125.8	79.1; 26.7
1B	K	DMSO[c]	69.4	165.4	111.5	70.4; 30.8
			(+28.7)	(−4.1)	(−14.3)	
2'B	Li	THF/HMPA (80:20)	74.0	166.5	114	nd;[f] 30.3
			(+31.3)	(−4)	(−13.1)	
4B	K	THF/toluene (50:50)	77.2	165	118.4	74.8; 29.8
			(+34.5)	(−5.5)	(−8.7)	
2B	Li	THF[d]	78.6	166.5	117.2	74.7; 30.0
			(+35.9)	(−4)	(−9.9)	
2B	Li	THF/hexane[d] (80:20)	78.7	167.0	117.4	73.7; nd or 74.7
			(+36)	(−3.5)	(−9.7)	
3B	Li	THF[d]	78.0	164.3	118.5	74.7; 29.5
			(+35.3)	(−6.2)	(−8.6)	
3B	Li	THF/hexane[d,e] (80:20)	77.1	163.1	120.4	73.7; nd or 74.7
			(+34.4)	(−7.4)	(−6.7)	

[a] $\Delta\delta$ = δ(anionic species) − δ(neutral precursor). [b] 1 M. [c] 0.33 M, 1.45 equiv of base used. [d] Spectrum run at 0 °C. [e] Small amount of a third species: CO 167.5. C_4 113.5. [f] nd = not detected.

to **1A** and **1B** and to **1A**,[M] and **1B**,[M] the *Z* geometry. The 8b, ν(C···O) mixing, on which the *Z* geometry assignment relies, is confirmed by the frequency shift (Table II, entries 4 and 13).

In **1A**,[M] the methoxy perpendicular rocking mode $\rho_\perp(OCH_3)$, which is clearly identified in the 1115–1140 cm^{-1} region when not hidden by the cryptand absorptions, usually shows two components as well as the ν(C···O) and 19b modes. These frequency doublings may be assigned to the existence of two conformations around the C–OMe bond, s-cis and s-trans (or gauche), while the bulky *tert*-butyl **1B**,[M] enolate is probably only gauche as observed in the solid state for *tert*-butyl propionate enolate.[9]

Charge delocalization into the phenyl ring of these species, as estimated by the $^{13}C_4$ negative shift[41] (−14 ppm) (Table IV), is somewhat larger than in the phenylacetone enolate free ion[40] (−11 ppm) but significantly smaller than in other planar benzyl anions.[38,42-44] This is certainly due to the oxygen atom electronegativity, so that some negative charge remains on that atom. Such a phenomenon is also in line with the smaller shift to lower

Scheme II

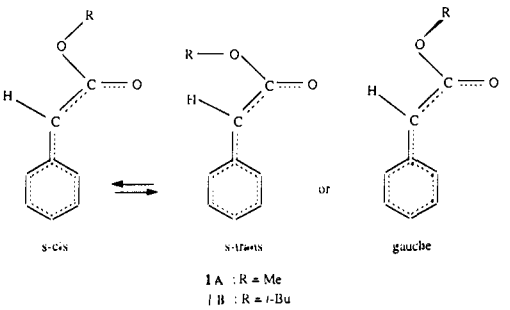

(42) (a) Peoples, P. P.; Grutzner, J. B. *J. Am. Chem. Soc.* **1980**, *102*, 4709. (b) Wen, J. Q.; Grutzner, J. B. *J. Org. Chem.* **1986**, *51*, 4220.

(43) Keys, B. A.; Eliel, E. L.; Juaristi, E. *Isr. J. Chem.* **1989**, *29*, 171 and references cited therein.

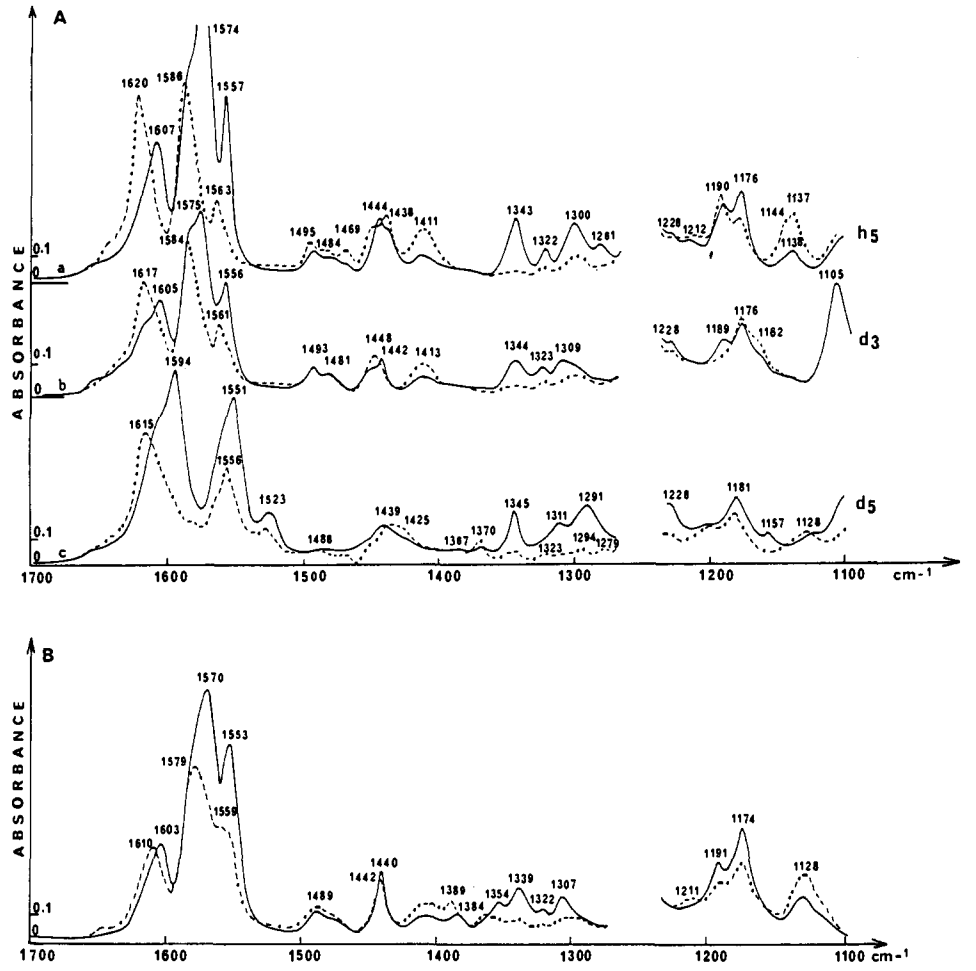

Figure 5. Infrared absorption spectra of carbanionic species **2A,Li** and **3A,Li** (Aa), **2A,Li-d_3** and **3A,Li-d_3** (Ab), **2A,Li-d_5** and **3A,Li-d_5** (Ac), and **2B,Li** and **3B,Li** (B) in THF solution, obtained respectively at a short or long time after their generation. The carbanionic species were generated with LHMDS. The spectra (—) observed at a short time after generation (approximately 15 min) correspond mainly to **2A,Li** or **2B,Li**. The spectra (- - -) observed at a long time after the initial spectrum. Δt = 7 h (a), 4 h 35 min (b), 6 h (c), and 1 h 45 min (B) correspond mainly to **3A,Li** or **3B,Li**. The spectrometer temperature varies from 26 to 32 °C.

frequency of the phenyl ring stretching modes 8b (−41 cm^{-1} for [PhCHCN]$^-$[38] versus −21 cm^{-1} for **1A**), while the 8a mode frequency shift is similar in both cases (−21 and −18 cm^{-1}, respectively). The higher ν_a(C–C–C) or "e" mode frequencies observed at 1400 cm^{-1} for **1A** or 1411 cm^{-1} for **1B** instead of 1373 cm^{-1} for [PhCHCN]$^-$[38] are coherent with this smaller electronic delocalization. Furthermore, the planarity of the enolate system[41] is confirmed by the **1A**,[Li] $^1J_{CH}$ value (150.8 Hz).

THF-Solvated Tight Ion Pairs and Aggregates: 2A,Li and 3A,Li or 2B,Li and 3B,Li. Two lithiated species **2A,Li** or **2B,Li** and **3A,Li** or **3B,Li** could be observed by IR and NMR when **A** or **B** was treated by LHMDS in THF. **2A,Li** or **2B,Li** appeared when the spectra were run immediately after the addition of base to the neutral precursor (Figures 2 and 5); these species are characterized (Figures 2 and 5) by a large intensity of the absorption at 1574 cm^{-1} for **2A,Li**, 1570 cm^{-1} for **2B,Li** (Table I, entry 2, and Table III, entry 3), and 1551 cm^{-1} for **2A,Li-d_5** (Table I, entry 9), assigned to the 8a mode. The ν(C···O) mode located at 1607, 1603, and 1594 cm^{-1} and the 8b mode at 1557, 1553, and 1523 cm^{-1} for **2A,Li**, **2B,Li**, and **2A,Li-d_5**, respectively, give less intense bands. These bands slowly disappeared with time (up to a few hours, Figure 2) at the benefit of those due to species **3A,Li**, **3B,Li**, and **3A,Li-d_5**, which are characterized by large intensities and broader absorptions at 1586, 1579, and 1556 cm^{-1}, respectively (Table I, entry 10), also assigned to the 8a mode; the ν(C···O) at 1620 or 1610 cm^{-1} and the 8b mode at 1563, 1559, and 1527 cm^{-1} are less intense.

Therefore, as the 8a mode intensity is the most enhanced (vide supra), all of these enolate species exhibit the *E* configuration. After a few hours, **3A,Li** was highly predominant, regardless of the concentration of the solution (0.25–0.025 M, Figures 2 and 3). Different behavior was observed with the *tert*-butyl ester enolate (Figures 2 and 3): at 0.25 M concentration, **3B,Li** became predominant although to a lesser extent, in solution after 1 h and 45 min. The same **2B,Li**/**3B,Li** mixture was observed immediately after the generation of the *tert*-butyl enolate by *n*-BuLi in THF/hexane (80:20, v:v). However, dilution to 0.05 M concentration (Figure 3) increased the relative amount of **2B,Li**. These dilution experiments show that the **2B,Li** and **3B,Li** species are in equilibrium, which can be displaced toward **2B,Li** by dilution with THF. From these observations, a solvated monomeric tight ion pair structure is assigned to **2B,Li** and a dimeric one to **3B,Li**, the equilibrium being mainly entropy driven.[16,45] Indeed, the equilibrium is more rapidly reached when the solution is heated to 36 °C. These assignments rely on Streitwieser's previous results[21] implying that lithium *tert*-butyl phenylacetate enolate **B,Li** is monomeric in 10^{-3} M THF solution. In the methyl ester case, in connection with the spectral similarities of the **A,Li** and **B,Li** species, **2A,Li** should be a monomeric tight ion pair and **3A,Li** a dimeric one, whose greater stability could be due to the small

(44) (a) Bottin-Strzalko, T.; Seyden-Penne, J.; Pouet, M. J.; Simonnin, M. P. *J. Org. Chem.* **1978**, *43*, 4346. (b) Denmark, S. E.; Dorow, R. L. *J. Am. Chem. Soc.* **1990**, *112*, 864.

(45) (a) Kim, Y. H.; Paoli, D.; Chabanel, M. *C. R. Acad. Sci. Paris Ser. C* **1985**, *301*, 1113. Chabanel, H. *Pure Appl. Chem.* **1990**, *62*, 35. (b) *Carbanion, living polymers and electron transfer processes*; Szwarc, M., Ed.; Interscience: New York, 1968; Chapter 8.

Scheme III

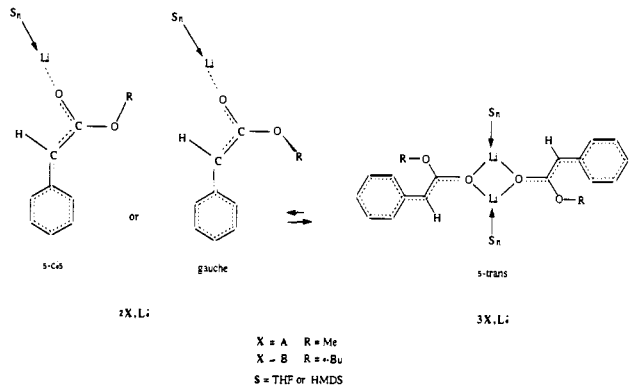

size of the methyl group and conformational effects. Enolate generation by LHMDS induces the formation of an HMDS-solvated monomer whose dimerization is certainly slower than when *n*-BuLi in the presence of hexane is used.

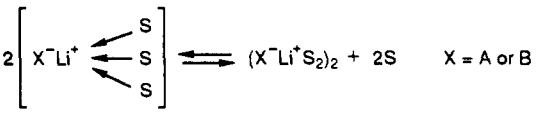

In **2A,Li** and **3A,Li**, similar to the previous observations for **1A**, some modes such as 19a, 19b, or $\rho_\perp(OCH_3)$ (or $\rho_\perp(OCD_3)$ in the d_3 species) show two components (Table I, entries 2, 3, 5, and 6), while in **2B,Li** and **3B,Li** they do not. This is indicative of the presence of two conformers around the C–OMe bond. Furthermore, in the ^{13}C NMR a negative $\Delta\delta$ shift of the OCH_3 carbon is observed for **2A,Li** (−1.6 ppm) and a positive one for **3A,Li** (+2.3 ppm) (Table IV), indicating that the two conformations should not be as populated in both entities. The s-cis conformer, responsible for the negative OCH_3 shift, might be more populated in the monomeric tight ion pair **2A,Li**, relative to the s-trans or gauche one, inducing a positive OCH_3 shift; the reverse should occur for the dimeric one, **3A,Li**, probably to avoid steric hindrance. In **2B,Li** and **3B,Li**, a single gauche conformer should be present. However, due to the bulkiness of the *t*-Bu group, dimeric **3B,Li** should be less stable than **3A,Li** relative to the corresponding monomer **2B,Li** or **2A,Li**.

Charge delocalization into the phenyl ring, as estimated by $\Delta\delta^{13}C_4$ variations, is less important in **2A,Li** or **2B,Li** and **3A,Li** or **3B,Li** (−7 to −10 ppm) than in **1A** or **1B** and **1A,[M]** or **1B,[M]** species (−13.9 to 15 ppm) (Table IV). This is due to the strong O^-Li^+ interaction within the tight ion pairs. In dimeric **3A,Li** or **3B,Li**, the electronic delocalization ($\Delta\delta C_4$: −7 and −8.6 ppm) is smaller than in **2A,Li** or **2B,Li** (−9.4 and −9.9 ppm); this result is in agreement with Jackman's previous findings[16,17] related to aryl amides or aryl ketone enolates showing the sensitivity of ^{13}C NMR to the degree of aggregation, with less aggregated species exhibiting higher C_4 upfield shifts. This difference in delocalization between **2A,Li** or **2B,Li** and **3A,Li** or **3B,Li** as well as the difference in $\nu(C\cdots O)$ frequency lowering is in line with the proposed Li double-bridged structure of the dimeric species (Scheme III), rather than a dipolar antiparallel stacking of the ion pairs. It is worth quoting that, in the present case, the exchange between the different species **2A,Li** and **3A,Li** or **2B,Li** and **3B,Li** is slow at 0 °C on the NMR time scale, while for lithioisobutyrophenone aggregates this phenomenon, which involves dimers and tetramers, only takes place at lower temperatures.[18] However, slow exchange between monomers and dimers of lithiated amino nitriles has been recently observed in THF by Enders.[62] Furthermore, previous literature data implies that dimerization of lithium ion pairs can be slow.[45b]

From these assignments, it appears that lithium methyl and *tert*-butyl phenylacetate enolates exhibit an *E* configuration in THF which is similar to that of lithium propionate enolates in solution[8b,11] or in the solid state,[9] but differs from that deduced from silyl chloride trapping experiments[8a] (vide infra).

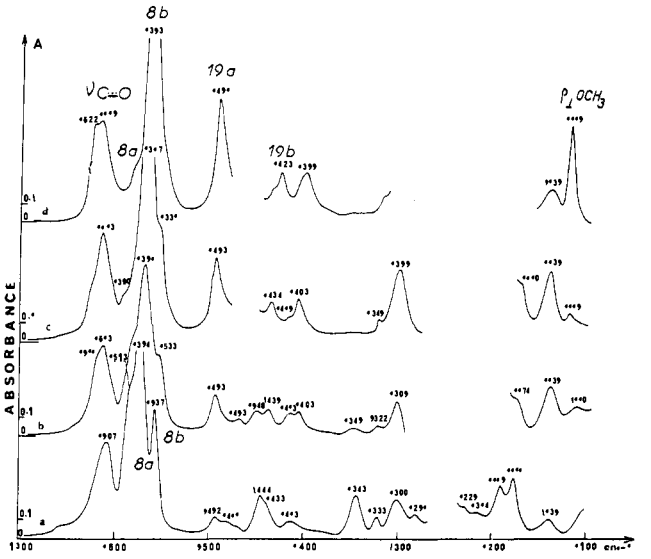

Figure 6. Influence of HMPA additions to a THF solution on the infrared absorption spectra of the carbanionic species **A,Li** generated with LHMDS. The different species are mainly the following: **2A,Li** in THF (a): **2'A,Li** in THF/HMPA (90:10, v:v) (b); **2'A,Li** in THF/HMPA (80:20, v:v) (c); **1A,[Li]** in THF/HMPA (32:68, v:v) (d). The concentrations are 0.25 M. The cell thickness is 0.003 cm. The spectra are obtained at 26 °C.

HMPA- or DMSO-Solvated Ion Pairs: 2'A,Li or 2'B,Li. The influence on the IR spectrum of the addition of progressive amounts of HMPA to a THF solution of **A,Li** or **B,Li** is reported in Figure 6, Table II, entries 8 and 5, and Table III, entries 9 and 7. The same spectra could be obtained when generating the enolates by LHMDS in the same solvent mixtures.

For small amounts of HMPA (≤10% v:v) (2 equiv of HMPA per Li) (Figure 6b), next to the absorptions due to **2A,Li** and **3A,Li** a new species **2'A,Li** appeared, whose absorptions are shifted to lower frequencies relative to those of the other species; **2'A,Li** became highly predominant when the THF/HMPA ratio was 80:20 (v:v) (4 equiv of HMPA per Li) (Figure 6c). For higher HMPA ratios, next to **2'A,Li** solvent-separated ion pairs **1A,[Li]** could be observed which were exclusively formed when the THF/HMPA ratio was 32:68 (Figure 6d). Similar behavior could be observed with **B,Li**. Two important features characterize the IR spectra of **2'A,Li** and **2'B,Li** compared to **2A,Li** and **2B,Li**: in **2'A,Li** the most intense mode is the 8b one (**2'A,Li**: 1567 cm^{-1}; **2'B,Li**: 1563 cm^{-1}) (Table II, entry 8, Table III, entry 9) while 8a is the most intense for **2A,Li** (Figure 6a). Therefore, **2'A,Li** and **2'B,Li** enolates exhibit the *Z* geometry.

The ^{31}P NMR spectra of solutions of **2'A,Li** and **2'B,Li** in THF/HMPA (90:10 and 80:20, v:v) (2 and 4 equiv of HMPA per Li) have been recorded at various temperatures (293–183 K). The spectrum of **2'A,Li** generated with LHMDS showed two ^{31}P signals at 183 K at δ 26.0 and 26.66 ppm (H_3PO_4 as external standard), the low-field signal being unresolved. The relative intensities of these signals were nearly 50:50 in the former case and around 40:60 in the latter one. The spectrum of **2'B,Li**, when generated with *n*-BuLi, in THF/HMPA (80:20) exhibited similar behavior; at 203 K, the low-field signal was a quartet as reported by Reich and Green[46] for HMPA-solvated organolithium compounds: $^2J_{PLi}$ was 8 Hz, and $\delta^{31}P$ signals were +26.08 (free HMPA) and +26.75 ppm (coordinated HMPA), both having the same intensity. The small difference in ^{31}P chemical shifts between free and Lewis acid coordinated HMPA has other precedents in the literature.[47]

(46) (a) Reich, H. J.; Green, D. P. *J. Am. Chem. Soc.* **1989**, *111*, 8729. (b) Reich, H. J.; Borst, J. P. *J. Am. Chem. Soc.* **1991**, *113*, 1835. Due to the fact that we observe a quartet in the ^{31}P NMR spectrum but an ill-resolved broad signal in the ^7Li spectrum, we cannot firmly assign that the species is a di-HMPA solvate. We are grateful to Prof. Reich for raising such an interpretation.

As in THF/HMPA (80:20), the ratios of the ^{31}P NMR signals for free and bonded HMPA are 40:60 and 50:50, respectively, for **2'A,Li** and **2'B,Li**. These results indicate that **2'B,Li** and probably **2'A,Li** too are monomeric contact ion pairs, externally solvated by HMPA; the solvation number is probably 2.[46]

Charge delocalization into the phenyl ring is larger in **2'A,Li** or **2'B,Li** ($\Delta\delta C_4$: −13 ppm) (Table IV) than in **2A,Li** or **2B,Li** (−9.4 or −9.9 ppm) due to the weaker interaction between the HMPA-solvated lithium cation and the anionic moiety; it is, however, less important than in the solvent- or cryptand-separated ion pairs **1A,[M]** or **1B,[M]** ($\Delta\delta C_4$: −15 ppm). This observation is in agreement with those of Jackman and Lange,[19] who noted that in HMPA-solvated lithium isobutyrophenone enolate there is a stronger interaction between the cation and the enolate moiety than in the solvent- or cryptand-separated ion pairs.

Contrary to Ireland's recent observations concerning to lithium propionate enolates,[8b] the addition of HMPA to a solution of monomeric or dimeric lithium phenylacetate enolates **2A,Li** or **3A,Li** and **2B,Li** or **3B,Li** (having, as we have assigned, the *E* geometry) induced an $E \rightarrow Z$ configurational change, next to the electron density reorganization due to Li solvation. This behavior is similar to that in Corey and Gross'[11] or Saunders et al.'s[14] reports on ketone enolates. Such an isomerization might imply a rapid reprotonation–deprotonation process due to the amine present in the medium, possibly as a Li cation ligand, when the enolates were generated with LHMDS; such an interpretation has some precedent in the literature.[4c,20,48,49] However, when HMPA was added to a solution of **2B,Li** or **3B,Li** generated using *n*-**Bu**Li, no amine was present and $E \rightarrow Z$ isomerization also took place. As it is well-known that HMPA is not a proton donor,[50] it seems likely that this fast isomerization involves, as intermediate species, free anions or relaxed ion pairs, which should be in equilibrium with externally solvated ion pairs. Such a process has been recently advocated by Jackman and Rakiewicz[51] to interpret exchanges between dimers and mixed dimers of various phenolates. When larger amounts of HMPA are added (THF/HMPA, 32:68), higher lithium solvates are generated, the cation then being surrounded by four HMPA ligands so that free anions or solvent-separated ion pairs **1A,[M]** or **1B,[M]** are characterized in the IR spectra.

From the IR spectra of the solutions of lithium methyl or *tert*-butyl phenylacetate enolates generated with LHMDS in THF/DMSO (27:73, v:v) (Table II, entry 6, Table III, entry 8), it appears that next to **1A,[Li]** or **1B,[Li]**, which are solvent-separated ion pairs, one might observe small amounts of another species, whose spectral characteristics are close to those of **2'A,Li** and **2'B,Li** in THF/HMPA. They should be DMSO externally solvated ion pairs. Indeed, the presence of Li-associated pairs in DMSO has precedent in the literature regarding acetoacetates[52] or phosphono ester[53] enolates.

Potassium-Associated Ion Pairs: 4A,K or 4B,K. When potassium enolates were generated with *t*-BuOK in DMSO, only solvent-separated ion pairs **1A,[K]** or **1B,[K]** were observed in the IR, in agreement with previous results on bidentate enolates.[52-54] However, when KHMDS in toluene was used to generate these enolates, ion pairing was expected in the associating medium (THF/toluene, 40:60, v:v). The IR frequencies of species **4A,K** and **4A,K**-d_5 so formed are in Table II (entries 9 and 15), while the IR frequencies of **4B,K** are in Table III (entry 11). Their ^{13}C NMR parameters are in Table IV.

In the IR, the frequencies of the $\nu(C\cdots O)$, 8a, and 8b modes are somewhat lower in **4A,K** than in **2A,Li** but are very close in **4B,K** and **2B,Li**. The most remarkable feature is that, in **4A,K** or **4B,K**, the relative intensities of the 8a and 8b modes are nearly equal, thus indicating the probable coexistence of *E* and *Z* geometrical isomers since in **2A,Li** or **2B,Li** the 8a mode was more intense.

In the NMR, $\Delta\delta C_4$ for **4A,K** (−8.7 ppm) is intermediate between **2A,Li** (−9.4 ppm) and **3A,Li** (−7.0 ppm) but of the same order of magnitude for **4B,K** and **3B,Li** (−8.7 and −8.6 ppm, respectively). $\Delta\delta C_\alpha$ is noticeably smaller (+25.5 ppm) in **4A,K** than in the two other species (**2A,Li**: +33.7 ppm; **3A,Li**: +29.3 ppm). However, when the parameters of **4B,K**, **2B,Li**, and **3B,Li** are compared, $\Delta\delta C_\alpha$ is nearly identical (+34.5, +35.9, and +35.3 ppm, respectively). K aggregates are therefore different from Li-associated species.

As in the lithium-associated species, progressive addition of DMSO to **4A,K** solutions induces the progressive appearance in the IR spectra of the absorptions due to **1A,[K]** solvent-separated pairs, which are thus in equilibrium with the K-associated tight ion pairs or aggregates.

Trimethylsilyl Ketene Acetal Formation. From our previous experiments, $E \rightarrow Z$ enolate isomerization takes place in the presence of HMPA. That is the reason why trapping experiments were performed in THF, by Me_3SiCl, without the addition of any cosolvent, which was necessary when trapping was done by *t*-$BuMe_2SiCl$.[8a] In order to compare our results with those of the literature,[2,8a,23,55] trapping experiments were also run after low-temperature generation of enolates, using *n*-**Bu**Li, LDA, or LHMDS as bases. The experimental processes were the following: addition of the ester to the base in the presence of an excess (6 equiv) of freshly distilled Me_3SiCl (method 1a); same procedure except Me_3SiCl was added after enolate generation (method 1b); addition of the base to the ester solution followed by Me_3SiCl (method 2). The ratios of ketene acetals (*Z*)-**5X** and (*E*)-**5X** were determined by ^1H NMR in a pyridine-d_5 solution of the crude reaction mixture. The *Z* vs *E* geometries were assigned by ^1H NOE differential experiments[4c,22] in the same solvent on **5A**; reciprocal enhancement of the signals at δ 3.52 ppm (OCH_3) or 4.80 ppm (vinyl H) was all that was seen. The *Z* configuration was therefore assigned to this isomer, while the *E* geometry was assigned to the other ($\delta(OCH_3)$ 3.58, δ(vinyl H) 4.87 ppm). These results confirm the previous assignments considering that the lower field vinyl proton belongs to the *E* isomer[2,8a,23,55] and are extended to **5B**.

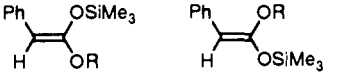

(*Z*)-**5X** (*E*)-**5X**

X = A, R = Me
X = B, R = *t*-Bu

The results of the trapping experiments are given in Table V. (*Z*)-**5X**/(*E*)-**5X** determinations were run immediately after quenching as it was observed, as already noted by other authors,[8b,12,23,55b,56] that the *Z*/*E* ketene acetal ratios could change with time. When enolate generation was run at −70 °C, our results were similar to those of Kiyooka et al.[2] under the same conditions (Table V, entry 1), but were slightly different when using predried LDA (entry 2) or LHMDS (entry 3); such observations do have precedent in the literature.[11,14,56,57] As also noted by Van Koten et al.[4d], the determined (*Z*)-**5X**/(*E*)-**5X** ratios (entries 6–13) do not reflect the highly predominant *E* geometry of the related

(47) Burford, N.; Royan, B. W.; Spence, R. E. V. H.; Cameron, T. S.; Linden, A.; Rogers, R. D. *J. Chem. Soc., Dalton Trans.* **1990**, 1521.
(48) Smith, J. K.; Bergbreiter, D. E.; Newcomb, M. *J. Org. Chem.* **1985**, *50*, 4549.
(49) Gaudemar, M.; Bellassoued, M. *Tetrahedron Lett.* **1989**, *30*, 2779.
(50) Normant, H. *Bull. Soc. Chim. Fr.* **1968**, 791.
(51) Jackman, L. M.; Rakiewicz, E. F. *J. Am. Chem. Soc.* **1991**, *113*, 1202 and references cited therein.
(52) (a) Arnett, E. M.; Maroldo, S. G.; Schriver, G. W.; Schilling, S. L.; Troughton, E. B. *J. Am. Chem. Soc.* **1985**, *107*, 2091 and references cited therein. (b) Cacciapaglia, R.; Mandolini, L. *Tetrahedron* **1990**, *46*, 1353 and references cited therein.
(53) Bottin-Strzalko, T.; Corset, J.; Froment, F.; Pouet, M. J.; Seyden-Penne, J.; Simonnin, M. P. *J. Org. Chem.* **1980**, *45*, 1270.
(54) Gais, H. J.; Hellmann, G.; Lindner, H. J. *Angew. Chem., Int. Ed. Engl.* **1990**, *29*, 100.
(55) (a) Slougui, N.; Rousseau, G.; Conia, J. M. *Synthesis* **1982**, 58. (b) Rousseau, G. Personal communication.
(56) Wilcox, C. S.; Babston, R. E. *J. Org. Chem.* **1984**, *49*, 1451.
(57) (a) Martin, V. A.; Murray, D. H.; Pratt, N. E.; Zhao, Y.; Albizati, K. F. *J. Am. Chem. Soc.* **1990**, *112*, 6965. (b) Wu, H. Y.; Walker, K. A. M.; Nelson, J. T. *J. Org. Chem.* **1990**, *55*, 5074.

Table V. Z/E Ratio of Ketene Acetals

entry	starting ester X	solvent/base (t, °C)	method[b]	quenching t, °C	(*Z*)-**5X**/(*E*)-**5X**[a] (yield, %)
1	**A**[b]	THF/hexane/LDA (−70)	1a	−70	25/75 (>98)
2	**A**	THF/LDA (−70)	1a	−70	45/55 (80)
3	**A**	THF/LHMDS (−70)	1a	−70	60/40 (70)
4	**A**	THF/LHMDS (−70)	1b	−70	25/75 (75)
5	**A**	THF/LDA (0)	1b	0	80/20 (52)
6	**A**	THF/LHMDS (rt or −10, 10 min)	1b	0 or −70	90/10 (75)
7	**A**	THF/LHMDS (34, 1 h, 30 min)	1b	0	95/5 (80)
8	**A**	THF/LHMDS (34, 1 h, 30 min)	2	0	95/5 (70)
9	**B**	THF/hexane/*n*-BuLi (0, 15 min)	2	0	50/50 (85)
10	**B**	THF/hexane/*n*-BuLi (−70, 15 min)	2	−70	55/45 (80)
11	**B**	THF/LHMDS (0, 15 min)	2	−70	50/50 (75)
12	**B**	THF/LHMDS (0, 15 min)	2	0	62/38 (93)
13	**B**	THF/LHMDS (20, 3 h)	2	−70	37/63 (80)

[a] Determination by ^{1}H NMR. Completion to 100% is starting ester. Quenching by Me_3SiCl after Et_3N addition gives the same results. [b] Run in conditions similar to ref 2. Method 1a: base, $ClSiMe_3$, then ester was added. Method 1b: base, ester, $ClSiMe_3$. Method 2: ester, base, $ClSiMe_3$.

enolates **2A**,**Li** or **2B**,**Li** and **3A**,**Li** or **3B**,**Li** as deduced from the IR study. Our results, in line with previous ones in the literature,[4d,8b,11,14] again cast some doubt on the reliability of the Z/E geometrical assignments to enolates according to trialkylsilyl halide trapping experiments. Moreover, when the enolates were generated in the conditions under which the IR spectra were performed (entries 6–9 and 11–13), we always obtained nonnegligible amounts of neutral esters **A** or **B** next to enoxysilanes **5A** or **5B**, although the IR spectra of the corresponding enolates did not show the presence of any ester and the quenching was done under strictly anhydrous conditions. This observation is reminiscent of the recent results of Van Koten et al.,[4d] who also observed the presence of neutral amino esters when quenching related zinc enolates. Very recently, Vedejs and Lee[58] noted that, in the presence of Lewis acids such as Me_3SiCl, protonation of an amide enolate by a secondary chiral amine included in the lithium enolate aggregate could take place with a high yield. All of these results show the problems which arise in ester enolate chemistry.

Conclusion

Deprotonation of methyl or *tert*-butyl phenylacetates **A** and **B** by lithium- or potassium-associated bases generates enolates whose Z or E geometry and association depends upon the cation and the solvent. From IR spectroscopy, according to the 8a or 8b mode/δ(CO) coupling, the E or Z configuration is assigned. Z enolates are formed under the following conditions: K or Li/DMSO, Li/THF–HMPA (32:68), K[2.2.2]/THF as free ions, solvent-, or cryptand-separated ion pairs, and Li/THF–HMPA (80:20) as externally HMPA-solvated ion pairs. In THF or THF/hexane, Li (E)-enolates, which are contact ion pairs, likely exist as monomers and dimers in equilibrium in slow exchange at room temperature on the ^{13}C NMR time scale. Such a low aggregation degree, when compared with Li ketone enolates which are tetrameric in THF,[20] is probably due to charge delocalization into the phenyl ring as well as to steric hindrance in the *tert*-butyl ester enolate **B**,**Li**. Indeed, Ciula and Streitwieser[59] have recently noted that charge delocalization inhibits aggregation.

The $E \rightarrow Z$ isomerization of lithiated enolates does not take place in aliphatic series[8b] when HMPA is added to their THF solutions. In the present case, this isomerization is due to the easy charge delocalization into the aromatic ring; (Z)-enolates which are thermodynamically more stable, as in the ketone case,[14] can thus be formed.

The poor diastereoselectivity observed previously[15] in the Michael induced ring closure reaction of lithium phenylacetate enolates **A**,**Li** and **B**,**Li** with bromo esters **6** in THF thus cannot be assigned to the presence of a mixture of (E)- and (Z)-enolates, each one reacting as propionate ester enolates[3c] in a stereoselective fashion.

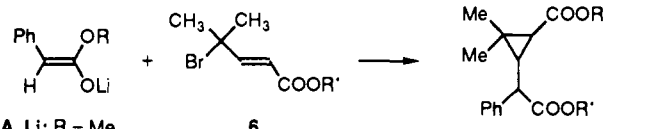

A, **Li**: R = Me
B, **Li**: R = *t*-Bu

6

mixture of stereoisomers

The (E)-enolate which has been characterized in the present work, therefore, reacts in a nonstereoselective way, due to its charge-delocalized structure, while propionate ester ones, which lead to stereoselective MIRC reactions, are more charge localized. Recent results of Corey and Lee[60] also show a similar trend when comparing the stereoselectivity of phenylacetate derivatives on the one hand and propionate ones on the other.

Experimental Section

Solvents and reagents were dried and purified prior to use. THF was distilled from sodium metal/benzophenone ketyl and kept under argon. DMSO, toluene, and HMPA were distilled over CaH_2 under inert atmosphere. $PhCH_2COOMe$ was commercial and distilled before use. $PhCH_2COOtBu$ was prepared according to ref 15b. Trimethylsilyl chloride was distilled over quinoline just before use; *n*-BuLi (1.6 M in hexane), LHMDS (1 M in THF), and KHMDS (0.5 M in toluene) are Aldrich commercial solutions. A silver nitrate test showed the absence of halides in *n*-BuLi and LHMDS solutions. *t*-BuOK (Merck) was doubly sublimed before use. CD_3OD was a CEA product. The purity of the reagents was previously checked by infrared spectroscopy; the presence of free amines or aromatic impurities could be easily detected. In such cases, the reagents were discarded. Each experiment was run at

(58) Vedejs, E.; Lee, N. *J. Am. Chem. Soc.* **1991**, *113*, 5483.
(59) Ciula, J. C.; Streitwieser, A. *J. Org. Chem.* **1991**, *56*, 1989.
(60) Corey, E. J.; Lee, D. H. *J. Am. Chem. Soc.* **1991**, *113*, 4026.
(61) Wenner, W. *J. Org. Chem.* **1950**, *15*, 548.
(62) Raabe, G.; Zobel, E.; Fleischhauer, J.; Gerdes, P.; Mannes, D.; Muller, E.; Enders, D. *Z. Naturforsch.* **1991**, *46a*, 275.

least three times with different reagent samples. Dry LDA was prepared by dropwise addition of 1.2 mmol of *n*-BuLi (1.6 M in hexane) to a stirred solution of 1.5 mmol of diisopropylamine freshly distilled over CaH_2 dissolved in 1 mL of THF at −10 °C. Following the addition the viscous mixture was stirred for an additional 10 min, after which time THF, hexane, and excess amine were removed under argon around 40–50 °C until a white powder was obtained. This powder was kept under argon.

Preparation of Deuterated Compounds. The following scheme was used.

(a) Methyl (Pentadeuteriophenyl)acetate (2A-d_5):

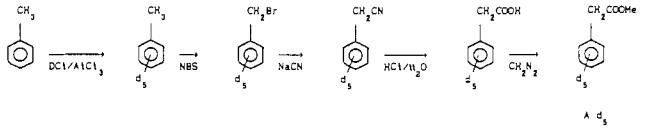

The synthesis of phenylacetonitrile has been previously described.[38] Hydrolysis of $C_6D_5CH_2CN$ was performed according to Wenner;[61] $C_6D_5CH_2COOH$ was then transformed into the corresponding methyl ester by CH_2N_2 in Et_2O. Isotopic purity was checked by ^1H NMR spectroscopy (*d* content ≥ 96%).

(b) Deuteriomethyl Phenylacetate (2A-d_3). Phenylacetyl chloride (7.7 g, 0.05 mol) was added dropwise to an ice–water bath cooled solution of CD_3OD (2 g, 0.05 mol, *d*% ≥ 99.8) in anhydrous cyclohexane (80 mL). The mixture was slowly heated to 60 °C and maintained at this temperature for 1.5 h. After the usual workup, the product was distilled (bp/14 mmHg: 104 °C; yield 6.2 g, 90%). and the isotopic purity was checked by ^1H NMR (≥95%).

Methyl (*E*)-4-Methylpentadien-2,4-oate. To a solution of 0.750 g (5 mmol) of methyl phenylacetate in 20 mL of DMSO was added, under argon atmosphere at room temperature, 0.580 g of nonsublimed *t*-BuOK. After 5 min of stirring, 1.03 g (5 mmol) of methyl 4-bromo-4-methylpenten-2-oate was added. After stirring for 30 min, quenching with aqueous saturated NH_4Cl solution followed by ether extraction, drying of the organic phases over $MgSO_4$, and evaporation, methyl 4-methylpentadien-2,4-oate was obtained; its spectral and GLC characteristics were similar to those previously described.[30] Similar results were obtained when starting from preformed $PhCH_2COOK$. When using disublimed *t*-BuOK, this reaction led, as previously described,[15b] to *anti*-methyl phenyl-2-(carboxymethyl)-3-methyl-5-hexen-4-oate.

Preparation of Solutions. All experiments were carried out under argon in a dry flask equipped with a rubber septum for the introduction of the reagents via a syringe. One millimole of starting ester (**A** or **B**) was dissolved into the required amount of solvent so that the final solution was 0.25 M; 0.05 and 0.025 M solutions were obtained by dilution of the 0.25 M one. To the magnetically stirred solution were added *n*-BuLi, LHMDS, or KHMDS (1.1–1.5 mmol) solutions by a syringe. The final solution was then stirred at room temperature for various times, and an aliquot was transferred under argon into the NMR tube or the IR cell in a glove-bag. *t*-BuOK was added to the solution under argon in a glove-bag.

IR and Raman Spectra. Infrared spectra have been scanned on a Perkin 983 spectrometer at the compartment temperature between 26 and 32 °C. The frequencies are given with a precision of ±1 cm^{-1} for sharp bands. Cell thickness was 0.003 cm for 0.25 M solutions and 0.02 cm for more dilute ones. They were equipped with CaF_2 windows, and the solvent spectra were subtracted from the solution ones.

Raman spectra were obtained using an RTI Dilor spectrometer. The 514.5 nm exciting radiation was provided by an argon ion laser with 300 mW power. The resolution was 2 cm^{-1}.

NMR Spectra. ^{13}C spectra were recorded on a Bruker AM 200 spectrometer. ^{31}P and ^7Li spectra and low-temperature experiments were performed on a Bruker AM 250 spectrometer. The temperature of the probe was 20 °C. ^{13}C, ^{31}P, and ^7Li spectra were determined by using the FT technique.

(a) ^{13}C NMR Spectra (50.33 MHz, 5-mm tube, ^2H lock). The ^2H resonance of D_2O contained in a capillary located inside the 5-mm tube provided the ^2H external lock. The carbon chemical shifts are reported in ppm downfield from tetramethylsilane. The proton-coupled ^{13}C NMR spectra were obtained by using the off-resonance technique, and the $^1J_{CH\alpha}$ coupling constant was determined by carrying out the NMR spectra without any decoupling.

(b) ^{31}P NMR Spectra (101.26 MHz, 10-mm tube, ^2H lock). A 5-mm tube filled with CD_2Cl_2 located inside the 10-mm tube was used for the ^2H external lock to perform low-temperature spectra recording. The ^{31}P chemical shifts are reported in ppm on the δ scale relative to a solution of pure H_3PO_4 as external standard.

(c) ^7Li NMR Spectra (97.20 MHz, 10-mm tube, ^2H lock). A 5-mm tube filled with a 0.6 M LiBr solution in CD_3OD was used both for the ^2H external lock and as an external standard. The low-temperature NMR spectra were recorded on a Bruker AM 250 spectrometer equipped with a variable-temperature unit. The sample was cooled under a nitrogen stream, and the probe temperatures were monitored with a thermocouple and are accurate to within 5 °C. For **4B**,Li (*n*-BuLi, THF/HMPA (80:20, v:v)) δ −0.48 ppm ($w_{1/2}$ = 31 Hz) at −83 °C.

Trapping of Enolates with Trimethylsilyl Chloride. (a) Method 1a. To a solution of 1.2 mmol LHMDS in 2.8 mL of THF (Table V, entry 3) or 2 mmol of hexane-free LDA[8a] dissolved into 4 mL of THF (Table V, entry 2) at −70 °C under argon was added slowly 6 mmol of trimethylsilyl chloride. One millimole of ester was then added dropwise by syringe. The solution was stirred at −70 °C for 10 min and was then allowed to warm to room temperature. After 15 min, the solvent and excess trimethylsilyl chloride were removed under reduced pressure. The flask was refilled with argon, and the residue was dissolved into 1.5 mL of pyridine·d_5 and examined by ^1H NMR.

(b) Method 1b. LHMDS or dry LDA (1.2 mmol) was dissolved under argon at room temperature in an appropriate amount of THF, so that the final volume was 4 mL. Then, 1 mmol of ester was added dropwise by a syringe at different temperatures (Table V, entries 4–7). Unless noted otherwise, the anion formation time was 10–15 min. The solution was cooled at 0 or −70 °C, and 6 mmol of trimethylsilyl chloride was added slowly by a syringe. After 10 min, the solution was allowed to warm to room temperature. Further treatment was as in method 1a.

(c) Method 2. The same amounts of reagents were used as in method 1b. The base, *n*-BuLi or LHMDS, was added dropwise by a syringe to the ester solution, so that the final volume was 4 mL in conditions described in Table V (entries 8–13). Addition of trimethylsilyl chloride and treatment of the reaction were performed as in method 1b.

Acknowledgment. We thank Mr. J. M. Dedieu for running ^{13}C, ^{31}P, and ^7Li NMR spectra, Mr. J. C. Merienne for determining the NOE effects, and Prof. G. Van Koten for the communication of the thesis of Dr. F. H. Van der Steen.

Supplementary Material Available: Figures VII–XI of carbanionic species **1A**,**K**, **1A**,**K**-d_5, **1B**,**K**, and **1B**,**Li** in THF, **4A**,**K**, **4A**,**K**-d_5, and **4A**,Li in DMSO, and **2B**,Li and **3B**,Li generated with *n*-BuLi and Tables VI–IX of IR frequencies and complete assignments of **B**, **B**,**M**, **A**, **A**,**M**, **A**-d_5, **A**,**K**-d_5 and ^{13}C NMR data of **A**,**M** and **B**,**M** (C_1, C_2, C_6, C_3, C_5) (11 pages). Ordering information is given on any current masthead page.